

## Research Article

### Fracture Properties of Glass Fiber Composite Laminates and Size Effect

Y. Mohammed<sup>1</sup>, Mohamed K. Hassan<sup>1</sup>, Abu El-Ainin H<sup>2</sup>, A. M. Hashem<sup>1</sup><sup>1</sup>South Valley University, Qena, Egypt, 83521<sup>2</sup>Minia University, Minia, Egypt, 61111

#### \*Corresponding author

Y. Mohammed

Email: [mohammed\\_yahya42@yahoo.com](mailto:mohammed_yahya42@yahoo.com)

**Abstract:** The fracture properties like fracture toughness and nominal strength of glass fiber reinforced epoxy laminates are very important especially when using cohesive zone model. Compact tension specimen test for  $[0, 90]_{2s}$  and center cracked specimen tension test for Quasi-isotropic laminates  $[0/45/90]_{2s}$  and  $[0/45/90/-45]_s$  are carried out. The open hole tension test is performed on a matrix of specimen of various diameters (2, 4, 6, 8 and 10 mm) keeping the hole diameter to width ( $d/w$ ) equal 1/6. The fracture toughness of cross ply laminates is measured as  $51.98 \text{ KJ/m}^2$  whereas, for Quasi-isotropic laminates  $[0/45/90]_{2s}$  and  $[0/45/90/-45]_s$  are  $32.98$  and  $31.5 \text{ KJ/m}^2$  respectively. A strength reduction of 32 % is observed with increasing the hole diameter from 2 mm to 10 mm, while this percentage was decreasing by inserting an angle ply as 26 % for  $[0/45/90]_{2s}$  and 14 % for  $[0/45/90/-45]_s$ . Delamination are observed with thickness increasing for un-notched specimens. Fiber orientation affects deeply the laminates carrying capacity.

**Keywords:** Nominal Strength, Fracture toughness, Quasi-isotropic laminates, Glass fiber reinforced epoxy

#### INTRODUCTION

Composite material has been widely applied in industry, military structure and Marine. Also analytical and numerical model such as; cohesive zone model which is basely depended on two main parameters which are un-notch nominal strength and fracture toughness of the material [1-5]. Therefore, the precisely experimental evaluation of the mechanical properties of this material is very important for used in design, modeling and simulation [5, 6] Pinho et al. [7] investigated the fracture toughness of carbon fiber reinforced laminates using compact tension test and compact compression test specimens. It is concluded that the initiation and propagation fracture toughness of the cross ply laminates  $[0, 90]_{8s}$  are determined as  $91.6 \text{ kJ/m}^2$  and  $133 \text{ kJ/m}^2$  respectively and for fiber compressive kinking, an initiation value of  $79.9 \text{ kJ/m}^2$ . It is used especially costly equipments. Donadon et al. [8] studied the tensile fiber fracture toughness characterization of hybrid plain weave composite laminates using non-standardized Over height Compact Tension (OCT) specimen. Initiation and propagation values around  $100 \text{ kJ/m}^2$  and  $165 \text{ kJ/m}^2$ , respectively, were obtained for the fiber toughness using the compliance method. It was found that the application of the ASTM E399-90 is fully questionable for composites in general and it can overestimate the toughness values if used in its original form. Three-point bend specimens with a  $(0)_{40}$  layup to measure fracture toughness of carbon PEEK composite, and surmised a mode I critical energy release rate of  $26 \text{ kJ/m}^2$ . The technique used to introduce a pre-crack in the specimen was not discussed by the authors [9]. A center notched compression specimen was carried out [10, 11, 12]. Many length of notch were used to study its effect on the fracture energy of T800/924C Carbon fiber reinforced epoxy

laminates with  $[0, 90, 0]_{3s}$  layup the critical energy release rate for the laminate was reported as  $38.8 \text{ kJ/m}^2$  and no effect for crack length on the fracture toughness. Camanho et al. [13] performed series of center crack specimen tension tests on different lay up of carbon fiber reinforced epoxy to validate the proposed analytical model without illustration the damage mechanics or failure mechanics induced in these techniques. The size effect or scaling effect which is the reduction of nominal strength with increasing of specimen size of carbon fiber reinforced polymer is investigated with a lot of authors [14-16]. Camanho et al [16] investigated the size effect of IM7-8552 carbon epoxy Quasi-isotropic laminates of  $[90, 0, 45, -45]_{3s}$  stacking sequence. It is reported that there is a clear size effect based on strength as large specimen decreases strength, but they don't investigate how to overcome this phenomena. The Glass fiber reinforced epoxy has an importance like carbon fiber. It has application in automobile industry, aerospace [6-16] and in Seawater Pipe System Offshore [17]. Therefore, the fracture properties of glass fiber reinforced epoxy laminate should be given a considerable investigation with more accuracy as there are very a little study which deal with fracture energy and size effect.

The main goals of the present study is to measure the very important fracture properties which is known as the fracture toughness for both cross ply of  $[0, 90]_{2s}$  and Quasi-isotropic of  $[0/45/90]_{2s}$  and  $[0/45/90/-45]_s$  glass fiber reinforced epoxy laminates. The size effect is investigated for these types of materials. Also a simple in plane shear test method will be illustrated to measure the in-plane shear modulus. A solution for the size effect defects has been suggested.

**MATERIAL AND EXPERIMENTAL PROCEDURES**

Glass fiber reinforced laminate of  $[0/90]_{2s}$ ,  $[0/45/90]_{2s}$  and  $[0/45/90/-45]_s$  stacking sequence using hand layup technique [18] are used where fiber bundles warping over a molding frames of equally step bolts using hand layup techniques, the curing process were on the room temperature. The material constitute properties are shown in tables 1 and 2. The fiber volume fracture is calculated using the ignition technique according to BS 3691. It is found 34%. The elastic properties and strengths of the unidirectional lamina are measured using ASTM D3039 test standers [19]. Five specimens are used for each test performed. The mean measured values of the ply elastic properties are listed in Table 3. While the in-plane shear modulus was obtained using  $\pm 45^\circ$  tensile in-plane shear test method which will illustrated in the next paragraphs.

**Table 1 the constituent materials of the composite laminates (CMB international Co.)**

Material	Type
Matrix	Resin-Kemapoxy(150RGL)
Reinforcement fiber	E-glass (Alkialian)-roving-pl=2200 gm/km

**Table 2 Mechanical and physical properties of E-glass fiber and epoxy resin, [20,21,22]**

Properties	E-glass	Kemapoxy(150RGL)
Density(kg/m <sup>2</sup> )	2540	1.07 ±0.02 kg/litres
Tensile strength (MPa)	2000	50-100
Tensile modulus (GPa)	76	1.2-4.5
Passion ratio	0.25	0.37-0.39

**Table 3 Ply elastic properties**

property	Mean value
Longitudinal young's modulus, $E_1$ (GPa)	27
Transverse young's modulus, $E_2$ (GPa)	5.3
In-plane shear modulus, $G_{12}$ (GPa), ( $\pm 45^\circ$ shear test)	1.75
Major passion ratio, $\nu_{12}$	0.31
Longitudinal strength ( $X_t$ ), MPa	645
Transverse ( $Y_t$ ), MPa	15

**$\pm 45^\circ$  tensile in-plane shear test method**

In this shear test method, a  $[\pm 45^\circ]_{2s}$  laminate is loaded in axial tension to determine the in-plane shear properties. This test method is frequently used because the specimens are easy to be fabricated and no special test fixture is required, the specimen is shown in Fig. 1. It is a simple test method for predicting in-plane shear modulus with an acceptable precision [23]. However, the laminate is not in a state of pure in-plane shear

stress [24]. Thus, the calculated shear stress and strain values at failure should only be used with caution. There are several test standards/guides based on this test method, i.e., ASTM D3518 [25].

The  $\pm 45^\circ$  tensile specimen has the following merits: good reproducibility, simple to make, is a conventional tensile test, economical in material requires, simple data reduction and is easy to test at high or low temperatures. The cross-ply  $[0, 90]_{2s}$  laminate was cut at  $45^\circ$  to gives the  $\pm 45^\circ$  tensile in-plane shear test of stacking sequence  $[45,-45]_{2s}$

The quasi-static tensile tests were done in a displacement-controlled manner with a displacement speed of 2 mm/min, during which the force F, the longitudinal and transverse strains,  $\epsilon_{xx}$  and  $\epsilon_{yy}$  were recorded. With these values, the shear stress  $\tau_{12}$  and shear strain  $\gamma_{12}$  can be calculated as:

$$\tau_{12} = F / 2wt \tag{1}$$

$$\gamma_{12} = \epsilon_{xx} - \epsilon_{yy}$$

Where w is the width of the specimen and t is the thickness. The longitudinal and transverse strains are measured using two perpendicular-element strain gauges (Model, FLA-6-11 of gage factor 2.1). Fig. 2 show the digital strain meter attach with the specimen, in the machine grippes.

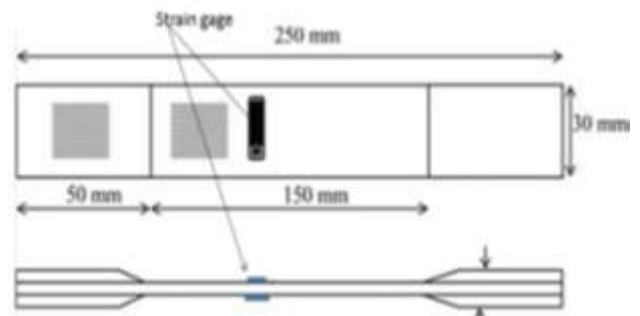


**Fig. 1  $\pm 45^\circ$  tensile in-plane shear test standard specimen**



**Fig. 2 tension Specimen between the machines**

**Compact specimen tension test**

1. This test methods is carried out according to ASTM E399 [26]. The specimen for fracture toughness testing is Compact Tension. It was machined from the laminates in accordance with the dimension given in ASTM E399 as shown in Fig.3.

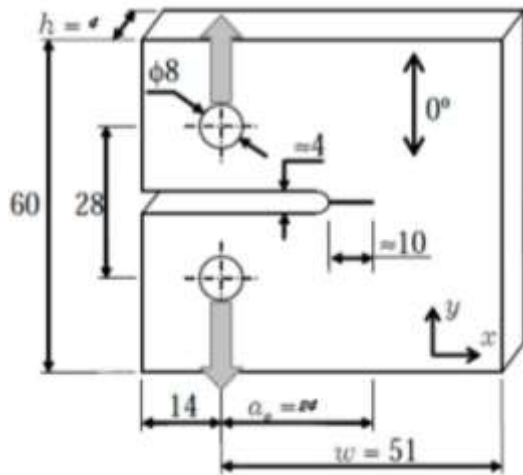


**Fig. 3 Typical CT specimen with dimension (dim. in mm)**

The initial portion a V notch has to be machined with a milling cutter or with a diamond saw and a starter crack has to be introduced at the root of the notch by tapping or sawing a fine razor blade [7]. The pre-cracked fracture specimen is loaded with suitable loading devices. For Compact tension specimen a loading clevis is required as shown in Fig. 4, special care is taken to create the loading holes to prevent delimitation and damage, therefore, they were cut using carbide tungsten drill while clamping the specimen between two sacrificial glass/epoxy plates of the same material. The fracture loads  $P_Q$ , obtained from the tests

of five specimens are used to determine  $K_{Ic}$  values ( $MPa\sqrt{m}$ ) as a measure of fracture toughness by using the following data reduction scheme. According to ASTM standard E399 [26], valid for an isotropic material, the critical stress intensity factor for a fracture load  $P_Q$ , is given by

$$K_{Ic} = \frac{P_Q}{h\sqrt{w}} f(a/w) \tag{2}$$

Where  $h$  = specimen thickness, mm,  $W$  = specimen width, mm,  $a$  = crack length, mm and  $f(a/w)$  is shape correction factor.

$$f(a/w) = \frac{2+a/w}{(1-a/w)^{1.5}} \left[ 0.886 + 4.64(a/w)^3 + 14.72(a/w)^3 - \right]$$

where  $h$  is the thickness of the specimen,  $w$  is the dimension from the load line to the right hand edge of the specimen, as indicated in Fig. 3 and  $a$  is the crack length, whose initial value  $a_0$  is also indicated in Fig. 3. The critical energy release rate of the laminate can be calculated from  $K_{Ic}$  as [7]:

$$G_{Ic} = J_{Ic} = \frac{K_{Ic}^2}{\sqrt{2E_x E_y}} \sqrt{\frac{E_y}{E_x} + \frac{E_y}{2G_{xy}} - \nu_{xy}} \tag{4}$$

Where  $E_x$ ,  $E_y$ ,  $G_{xy}$  and  $\nu_{xy}$  are the Young's moduli in the  $x$  and  $y$  directions (see Fig. 3), the shear modulus and the Poisson's ratio of the laminate, respectively, these properties are determined experimentally in the previous steps.

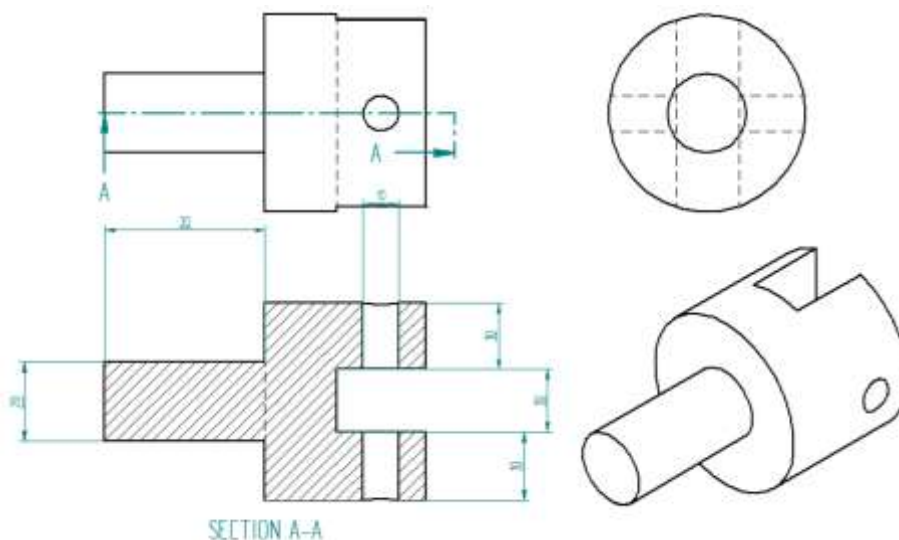


**Fig. 4 one part of the clevis used in compact tension test specimen**

The layup used is  $[90, 0]_{2s}$  of glass fiber reinforced epoxy laminates with the  $0^0$  direction is parallel to the loading direction as shown in Fig. 3. Five sample are used. Figure 5 shows the test set up. Fig. 6 shows the photograph of the compact tension test.



Fig. 5 Compact tension set up

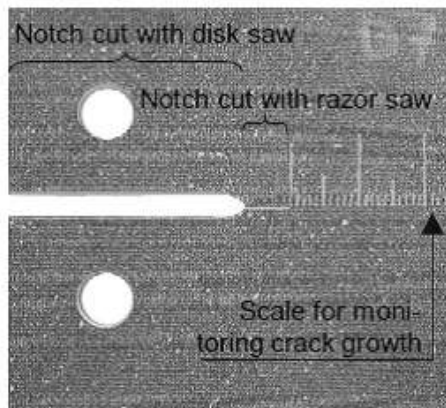


Fig. 6 Sketch of the compact tension test [7]

**Center crack plate specimen tension test**

The tension test of center crack plate specimen is carried out according to Soutis- Flick model [27] to measure the surface release energy of multidirectional composite laminates. The test is performed using the Quasi-isotropic laminates  $[0, -45, 90, 45]_s$  and  $[0/45/90]_{2s}$ . The manufacturing technique used in CT specimen is used. The specimen dimensions are shown in Fig. 6. Five specimens are used. The test is simple to be performed and can be summarized as follows:

1-Five specimen are used for tension test of the following nominal dimension; Width  $W=45$  mm, gauge section length-  $L=90$  mm, thickness-  $t=4$  for  $[0, -45, 90, 45]_s$  and  $t=7$  for  $[0/45/90]_{2s}$ , finally the center crack length  $-2a=15$  mm.(see Fig. 6).

2-After manufacturing the five specimens for each lay out, they loaded until failure and the specimen's failure load were obtained.

After measuring the failure load for each material the fracture toughness is measures as:

$$K_{IC} = \sigma \sqrt{\pi a} \sqrt{\sec\left(\frac{\pi a}{w}\right)}$$

Where (KIC) is the fracture toughness of the laminates, (a) is semi center crack length and (W) is laminates width. After substituting the specimen dimension in the equation the fracture toughness is calculated, then implemented in Eqn. 2.

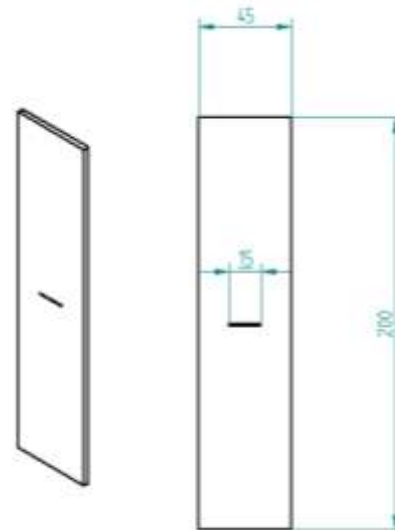


Fig. 6 Centered crack specimen un-notch tension test

The size effect needs to be compared with the un notch nominal strength of composite laminates; - (laminates without holes)-.Therefore the specimen which is shown in Fig. 7 is prepared. The nominal dimension is as follows:  $w=40$ ,  $L_g= 150$  and  $L= 250$  mm, the thickness  $t=4$  mm for 8 layers laminates or 7 mm for 12 layer laminates. Two-end tabs are attached in order to distribute the stress along the cross section of the specimen. Tension test is performed according to ASTM D638M-93 [28] standard to obtain tensile properties of plastic using five specimens and the nominal stress strain curve is drawn. The nominal un-notch strength is average of the five specimens. This test is performed on  $[0, 90]_{2s}$ ,  $[0/45/90]_{2s}$  and  $[0, 45, 90,-45]_s$  stacking sequence. The longitudinal displacement measured using a strain gage (2.1 gage factor), which is bonded on the surface of two of the specimens.



Fig. 7 Un notch composites coupon

**Open hole tension test for similar shape specimen**

The tension test of notched composite laminates is carried out to quantify the size effect and to obtain experimental data. The quasi-isotropic, cross ply and unidirectional laminates are of glass fiber/epoxy of stacking sequence [0, 90]2s, [0, -45, 90, 45]s and [0/45/90]2s. These are also to study the effect of stacking sequence on the size effect phenomenon. The unidirectional specimen is not tested for size effect, as it has no industrial application.

The presence of a stress raiser, in this case a circular hole, leads to enhanced complex damage and failure mechanisms, causing a wide range of effects not present in un-notched components. A matrix of specimens of different hole diameter and width are shown in Table 4, but all specimens keep that hole diameter to width ratio is constant ( $d/w = 1/6$ ) [29].

**Table 4 Experimental matrix program**

Diameter	Width	Ratio w/d	Number of specimen used
$d_1=2$	12	6	5
$d_2=4$	24	6	5
$d_3=6$	36	6	5
$d_4=8$	48	6	5
$d_5=10$	60	6	5

A typical specimen of end tab used in open-hole tensile tests is presented in Fig. 8. The displacement will be recorded with the machine load cell, as the fracture behavior during the test is important from fracture mechanics point of view.

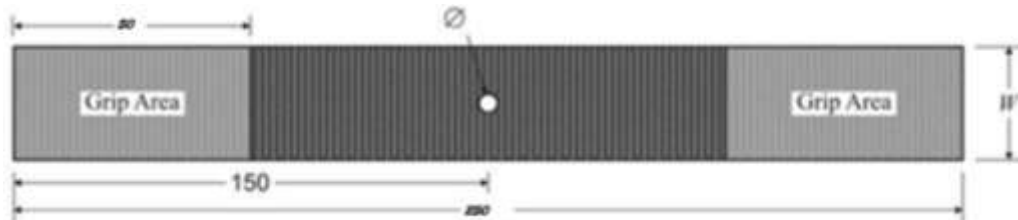


**Fig. 8 Typical OHT specimen with dimension**

**RESULTS AND DISCUSSION**

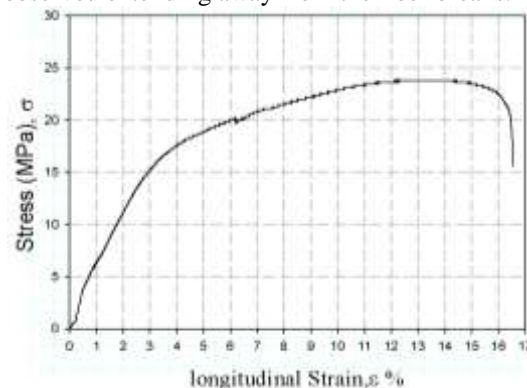
**Shear test**

Figure 9 shows stress-longitudinal strain curve for [45, -45]2s tension test specimen. This test is carried out to determine the shear strength and modulus of the material under consideration. Defining shear strength is still debatable as to which load value should be used [18, 30]. Bhatnager et. al. [30] considers the first load drop to be the shear load responsible for material failure. Khashaba [18] defined shear strength as the ratio of the load just prior to the nonlinear behavior, to the cross-sectional area. Some investigators [30] defined the in-plane shear strength as the stress value corresponding to the ultimate load. The latter definition for shear strength is more suitable for nominal strength failure criteria [30]. Fig. 10 shows the relation between the shear stress and strains measured in both longitudinal and transverse direction. From this figure, the relationship between the shear stress  $\tau_{xy}$  and shear strain  $\gamma_{xy}$  is constructed as illustrated in Fig. 11. The values of the in-plane shear stress and strain are calculated from Eqn.1:

The longitudinal and transverse strains are measured using two perpendicular-element strain gauges (Model, FLA-6-11 of gage factor 2.1). Hence, the in-plane shear modulus has been determined from the slope of the shear stress-strain diagram at 0.5% as:

$$G_{12} = \frac{\text{shear stress}}{\text{shear strain}} = \frac{8.75}{0.5} \times 100 = 1750 \text{MPa} = 1.75 \text{GPa}$$

The in plane shear modulus has a reasonably acceptable value compared with the value obtained from constituent material and volume fracture based on lamination theory [32] as 2 GPa. With 12.5 % error which is accepted from scientific and industrial point of view [31]. Shear stress-strain curve has proportional behaviors in the beginning. Just beyond proportional limit, it becomes nonlinear due to the accumulation of matrix cracks. The specimens tend to deform nearly into ‘dog bone’ like shape Fig.12. Furthermore, it must be remarked that the narrowing of the specimen to the ‘dog bone’ like shape does not happen in a uniform manner over the entire specimen, but starts near the clamped ends and then gradually grows along the entire specimen length. A more severe delamination is observed extending away from the fiber breaks.



**Fig. 9 Tensile stress longitudinal strain curve for [45,-45]2s specimen**

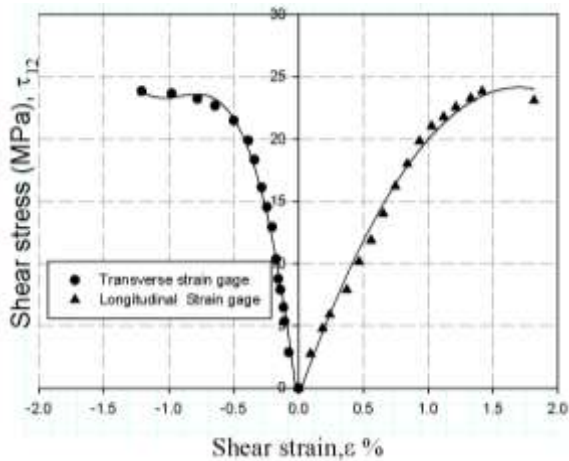


Fig. 10 Shear stress longitudinal and transverse strain curve for [45,-45]2s specimen

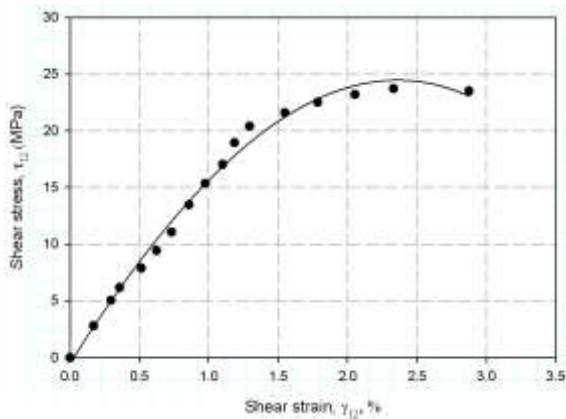


Fig. 11 Equivalent shear stress versus shear strain for [45,-45]2s specimen

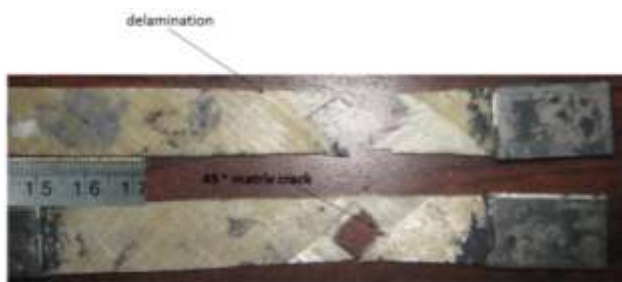


Fig. 12 Failure mode of [45, -45]₂s Shear test

**Compact tension**

For the Compact Tension specimen (CT) test, crack growth is neither smooth nor continuous: instead, several crack jumps of a few millimeters each time were observed, Fig.13. The fracture loads  $P_Q$ , obtained from the tests of five specimens and according eqns.2, 3 and 4 respects to the laminates elastic properties which are listed in Table 3 the fracture toughness  $K_{IC}$  values ( $MPa \cdot \sqrt{m}$ ) can be calculated. The average load value at 5% secant from the Fig. 13 equal 1900N, with the specimen dimension and total crack length ( $a_0+a_{FPZ}$ ), where  $a_{FPZ}$  is average fracture processing zone length and is shown in Fig. 14 and measured experimentally as approximately 3.5 mm. The average value as since

there is a tendency for the crack depth to vary through the thickness. Substituent these results in Eqn.2, the average fracture toughness  $K_{IC}$  is measured as;  $24.098 MPa \cdot \sqrt{m}$ , with stander deviation  $1.82 MPa \cdot \sqrt{m}$ . Substituent this value in Eqn. 4, fracture energy release rate  $G_{1c}$  is measured as  $51.915 kJ/m^2$  with the stander deviation is  $7.523 kJ/m^2$ .

Fig. 15 shows the post failure picture of the CT specimen, it is observed that the fiber bridging the two face of the crack and the crack advances straightly through the pre-crack direction, due to the highly stress intensity factor induced at the crack tip.

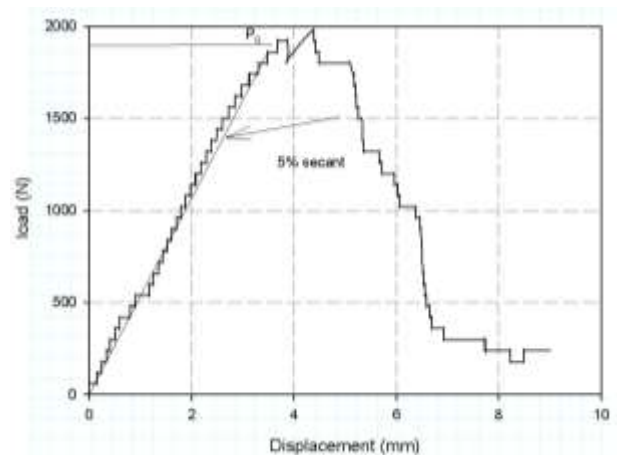


Fig.13 Typical load verse displacement curve

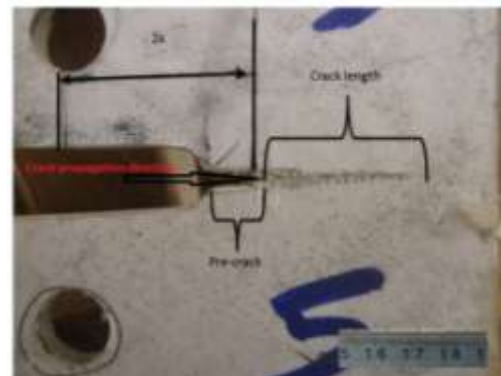


Fig. 14 the identification of the crack tip just before Maximum load



Fig. 15 Failure Mode of CT specimen

**Center crack specimen**

Soutis and Flek [27] showed that the fracture toughness of Quasi-isotropic laminates is independent of the center-crack size. Therefore, number of specimens that need to be tested is decreasing (only one length of the center crack was used). Figs. 16 and 17 show the load displacement curve for the test of center crack specimen, it is observed that the curve is smooth, a little jump seen, the extension records for laminate of stacking sequence [0/45/90/-45]<sub>s</sub> is less than that of [0/45/90]<sub>2s</sub> this return to the -45° plies which increase the shear stress action. The curve obtained from a compact specimen has a longer length compared to one obtained from a center-cracked specimen, because the gradient of K (stress intensity factor) in a compact specimen is decreasing whereas the gradient of K in a center-cracked specimen is increasing [27]. Fig. 18 shows the post-failure picture of one specimen for each stacking sequence of specimen. The post-failure load is determined from the load displacement curve for each laminates and with the help of Eqn.6, the failure stress is calculated and fracture toughness which are listed in tables 5 and 6. After measuring the failure stress for each specimen, the fracture toughness is determined by using the real dimension of the specimen:

$$\sigma_x = \frac{P_{max}}{A} \tag{6}$$

Where:  $\sigma$  = tensile strength, MPa,  
 $P_{max}$  = maximum load prior to failure, N,  
 $A$  = cross-sectional area, m<sup>2</sup>.

Then Substituting in Eqn. 5 the surface release energy can be calculated. The average value of the fracture toughness  $K_{IC}$  for [0/45/90]<sub>2s</sub> and [0/45/90/-45]<sub>s</sub> is 19.88 MPa.√m with Stander deviation 1.078 MPa.√m and 19.066 MPa.√m with stander deviation 1.2310 MPa.√m repetitively. Whereas, the fracture energies for these laminates are 35.48 Kj/m<sup>2</sup> with Stander deviation 3.763 Kj/m<sup>2</sup> for [0/45/90]<sub>2s</sub>, while for [0/45/90/-45]<sub>s</sub> is 32.57 kj/m<sup>2</sup> with stander deviation 2.417 Kj/m<sup>2</sup>. Fig. 18 (a) shows image of post failure surface of the center crack specimen of [0/45/90]<sub>2s</sub>. It can be reported that it is observed that the crack propagates through the notch corner and advanced approximately direct to the loading direction as the eight layer of 0° plies and the 90° plies are of highest stiffness more 45° plies which is the main reason for the shear band appearing in the fracture surface of Fig. 18 (b). It is appeared that matrix damage to take two forms. 1) crack in the 0° plies which

started at the ends of the slits, growing parallel to the 0° plies, through the specimen thickness and towards the gripping, 2) crack in the 45° fibers originating at slits 45° in addition, some cracking were observed between 0° plies and adjacent 45° plies. There is a more severe delamination was observed extending away from the fiber breaks. It is observed that the fiber mode of failure is tension mode with inclination angle about 45°, for angle ply and 90 for 0° ply. Focus look for Figs. 16, 17 it is shown that there is knee occurred at about 5kN this is because first 90° ply failure occurs.

The stacking sequence has a visible effect on notched failure strength and failure modes as an increase of angle plies -45° for laminates results in strength reduction approximately 7% as this angle layers introduce shear stress in both hole sides lift and right as shown in failure post image Fig.18

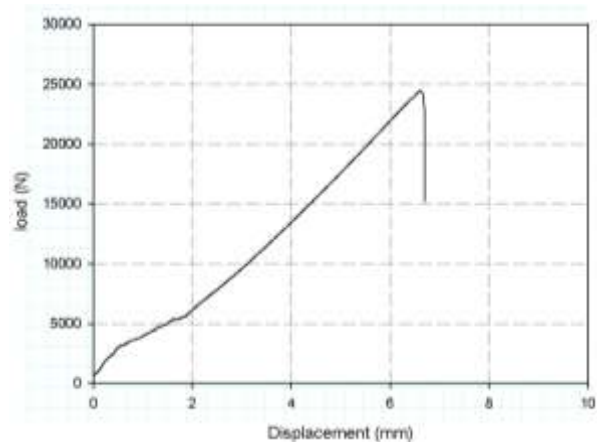


**Fig. 16 load displacement curve for (0, 45, 90)<sub>2s</sub>**

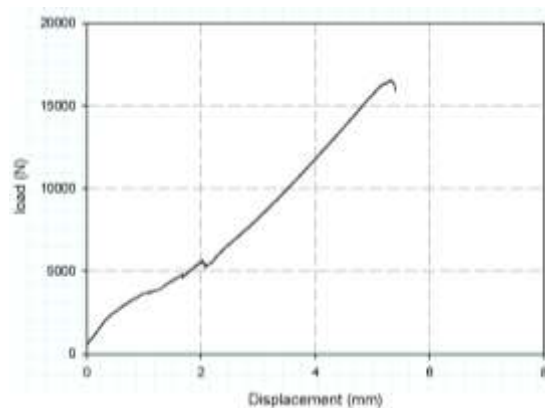


**Fig. 17 load displacement curve for (0, 45, 90,-45)<sub>s</sub>**

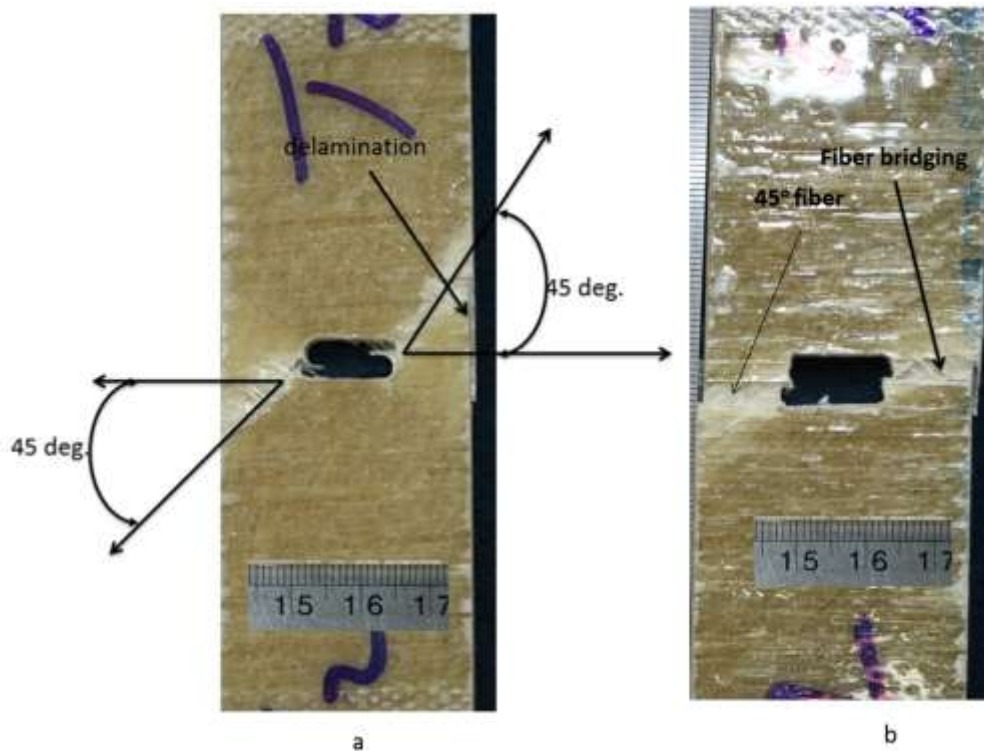


Fig.18 Failure modes for the centered crack composite laminates a)[0/45/90/-45]<sub>s</sub>, b)[0/45/90]<sub>2s</sub>

Table 5 Fracture toughness test results

Specimen number	(0,45,90) <sub>2s</sub>	(0,45,90,-45) <sub>s</sub>
	Stress (MPa)	Stress (MPa)
1	95.23	91.77
2	89.77	86.33
3	83.14	83.77
4	92.88	83.3
5	93.65	82.6

Table 6 Fracture Toughness and energy release rate

Specimen types	Fracture Toughness, K (MPa·√m)	Fracture energy, G <sub>IC</sub> (KJ/m)
[0/45/90] <sub>2s</sub>	19.88	35.48
[0/45/90/-45] <sub>s</sub>	19.066	32.57

### Un-notch Tension Test

Figure (20 a) shows the stress-strain diagram, of cross-ply glass fiber reinforced epoxy (GFRE) specimen, printed from the PC of testing machine in tension test as the machine draw the relation between load and displacement in time. The main characteristic of this curve is the knee at about 35 MPa. This knee was due to the failure of the transverse layers (90°) in the cross-ply laminates. Redistribution of stress between longitudinal fibers and matrix was occurred leading to another increasing in the tensile stresses with apparent tensile modulus lower than that for the initial linear portion. The final failure is catastrophic without any yielding.

Figure (20 b) show the stress-strain diagram obtained from the strain gage attached to the testing specimen. The actual modulus of elasticity was

calculated as 20.3 GPa at 0.5 % strain. This value is agreed with the theoretical results 21 GPa obtained using Micromechanical theories of lamina [32]. The un-notch average strength of five the cross ply laminates was calculated as 167 MPa with stander deviation equal 23.9 MPa. The failure mode is net tension with a little warping due to moment occurs, results from not perfect axially of fiber in 0° layer, also the failure mode tends to be near the gripping region in some specimen due to increase of stress concentration factor just above this region, matrix cracking with delamination near the fracture region through thickness.

The stacking sequences plays important role in the anisotropic material strength like this composite laminates. as the average strength for laminates of [0/45/90]<sub>2s</sub> is 94.75 MPa with stander deviation 6.5 MPa and it is decreases than [0/90]<sub>2s</sub> by about 43.3%

as shown in Fig. 21 and are listed in Table 7, this results is agree with the published results for other material laminated structure [33]. This can be attributed to that, the angle plies insert in the laminates produce shear stress across the fiber direction, which make a stat of complex stresses. Whereas the strength reduction not affected a lot with the addition of the -45 angle plies as the average strength of  $[0/45/90/-45]_s$  is 98.5 MPa with stander deviation 4.7 MPa. The shear stress in the direction of fiber is the main reason for strength reduction as clearly appear in the failure mode of  $[0/90]_{2s}$  which is due to pure tension and cracks are perpendicular to the loading direction (Matrix cracking), while for angle ply it is propagated along the fiber direction. It is clear from Table 7 and Figs. 21 and 22 that the brittleness decreases with insertion of angle ply for the laminates stacking sequence; this can be attributed to that, the laminates get some isotropy by inserting these angle to the material. Fig. 23 shows A more severe delamination was observed extending away from the fiber breaks, but no damage was visible during the tests. These results are by looking carefully to the failure region and noticing that the Surface 45° plies were completely delaminated. The edges of the specimens were also examined away from the fracture location and clear evidence of matrix cracking and delamination of the surface ply was found, as shown in Figure 20 b(b) for the smallest specimen, which is occurred before fiber failure. The specimens

presented different behavior: delamination occurred sooner and for more plies as the thickness increased. Failure was located near the tab ends with part of the material ejected, which suggests that stress concentration may be partly responsible for the failure. Failure combined also longitudinal splitting and fiber breakage.

Stiffness of the composite laminates is affected by stacking sequence as clearly shown in Figs. (20-b, 21 and 22) and values of Young's modulus which are listed in Table 7. Reduction of 46 % is occurred in stiffness of same number of layer from  $[0, 90]_{2s}$  to  $[0/45/90/-45]_{2s}$ . This reduction in modulus is attributed to yielding of the matrix in the 90° plies. This data indicates that laminate stiffness depends on the stiffness of the reinforcing fibers as well as the percentage of fibers aligned in the direction of loading, i.e. the stiffer laminates have a greater percentage of plies aligned with the direction of loading, as expected. Although, the laminates of 12 layer of stacking sequence  $[0/45/90]_{2s}$  have an equally aligned plies to  $[0, 90]_{2s}$  but decreases by about 30 % stiffness. This can be attributed to the increasing thickness in this laminates (7-9) mm for 5mm for cross ply laminates this increase in thickness induce stresses in this direction and the specimen can be in sate of tri-axial stress which reduced both stress and strength [34].

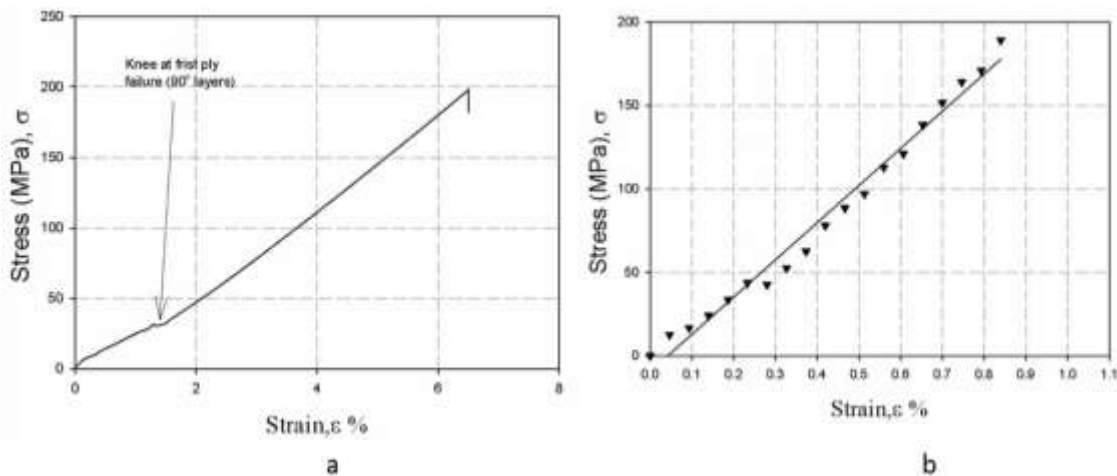


Fig.20 Stress strain relation for  $[0, 90]_{2s}$  a) Apparent strain b) Actual strain

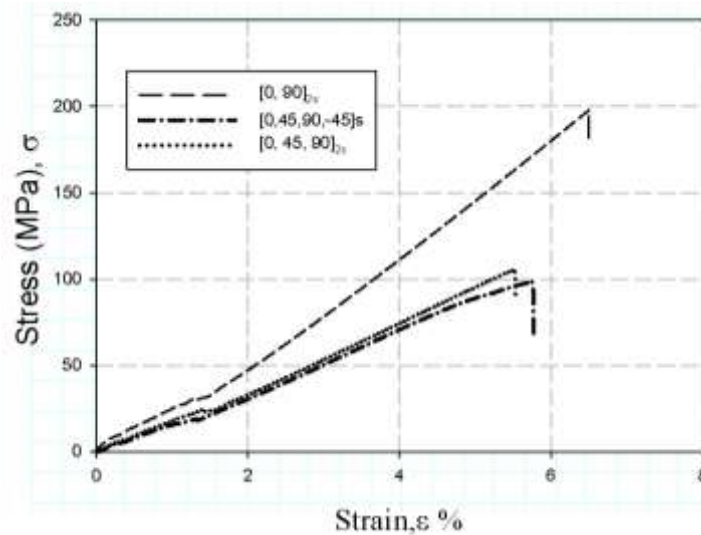


Fig. 21 Effect of stacking sequence on un notch nominal strength

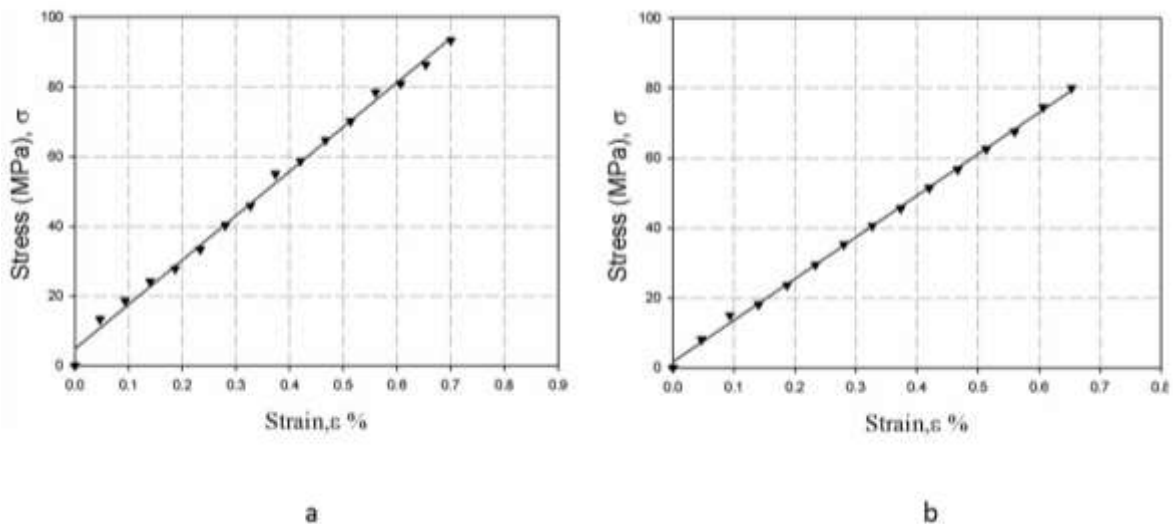


Fig. 22 Stress actual strains relation for a) [0/45/90]<sub>2s</sub> b) [0, 45, 90, -45]<sub>s</sub> stacking sequence

Table 7 Un notch strength of composite laminates

Stacking sequence	Mean nominal strength (MPa)	STDV (MPa)	Young's modulus (GPa) at 0.5 % strain
[0/90] <sub>2s</sub>	167.5	23.9	20.3
[0/45/90] <sub>2s</sub>	94.75	6.5	15
[0/45/90/-45] <sub>s</sub>	98.5	4.7	12

**Open hole Tension Test**

The experimental results presented in Table 8 and Fig. 24 clearly identify a specimen size effect: an increase in the hole diameter from 2 mm to 10 mm results in 29.5% a average reduction in the strength. The observed size effect is caused by the development of the fracture process zone, which redistributes the stresses and dissipates energy. In small specimens, the fracture process zone extends towards the edges of the specimen and the average stress at the fracture plane tends to the un-notched strength of the laminate. Size effect test results are listed in Table 8, the increase of size lead to increase of brittleness. The stress concentration at the hole is completely blunted. For this material it is, observed that the specimen failed

suddenly without visible damage due to the low interfacial toughness.

Figures 25 and 26 show the stress strain diagram for [0/45/90]<sub>2s</sub> and [0/45/90/-45]<sub>s</sub> composite laminates. It is show the same results that there is a specimen size effect appears for Quasi-isotropic laminates, but the size effect can be reduced by increasing numbers of 45° ply in the laminates stacking sequence with reducing the plate thickness. The 45° ply introduces shear stress around the hole that in role reduced the stress concentration factor and stress intensity factor. These angle ply make like stress releaser factor [7, 18]. Tables 9 and 10 show these results.

**Table 8 Test results for [0, 90]<sub>2s</sub> laminates open hole**

diameter	Mean nominal strength (MPa)	STDV (MPa)
2	135	4.12
4	121	3
6	116.25	5.8
8	105	3
10	95.5	1.11

**Table 9 Test results for [0/45/90]<sub>2s</sub> laminates open hole**

diameter	Mean nominal strength (MPa)	STDV (MPa)
2	86.25	3.3448
4	82.5	3.27
6	79.25	1.92
8	71	1.58
10	65.2	0.8672

**Table 10 Test results for [0/45/90/-45]<sub>s</sub> laminates open hole**

diameter	Mean nominal strength (MPa)	STDV (MPa)
2	68.84	1.29
4	67.35	3.96
6	67.27	4.755
8	62.3	2.87
10	57.75	3.25

The failure mode observed in all specimens is net-section tension as shown in Figs. 27,28 and 29. Damage mostly consists of matrix cracking in the ±45° and 90° plies in the vicinity of the hole, accompanied by some delamination around the hole; cracks in the 90° plies extend to the laminate edge. However, large triangular delamination zones emanate from the hole, decoupling plies and leading to rapid failure of the laminate. The shear band appears on surface inclined at 45° for GFRP [0/45/90/-45] at both side of hole, another words in direction of 45° fibers. Carefully look for crack propagation it is found that the crack path change direction a little before reach the specimen end. this because this location near the ends of 45° fiber, therefore fiber matrix debonding failure occurs and the crack propagates directly perpendicular to the load direction (Matrix cracking) as the inclined fiber cannot at this location resist the crack.

As the thickness increase a more severe delamination appeared in the structure which has dangerous damage for small size (small width respect to thickness) Fig.30 shows the delamination through thickness of [0/45/90]<sub>2s</sub> specimen thicker laminates.

Delamination occurs in combination with splitting at the notch, relieving the stress concentration [33].

Damage in the GFRP [0/90]<sub>2s</sub> laminate is characterized by axial splits at each side on the hole in the 0° plies. As the load increases, the damage zone increases in size, but the matrix cracks in the 90° plies only occur outside (i.e. towards the laminate edge) of the 0° ply axial splits indicating that the splits effectively blunt the stress concentration from the hole. The apparently lower level of matrix cracks in the 90° plies in the GFRP OHT specimens may be due to the less brittle nature of the matrix material. The failure mode changed from fiber-dominated to matrix-dominated with decreasing hole diameter, and that change was accompanied by an increase in delamination and much less change in strength with hole size than expected on the basis of the Whitney-Nuismer or Mar-Lin hole size models. It is attributed to change of the failure mode to the interlaminar stresses in the region around the hole boundary, which decrease with increasing ratio of hole radius to laminate thickness.

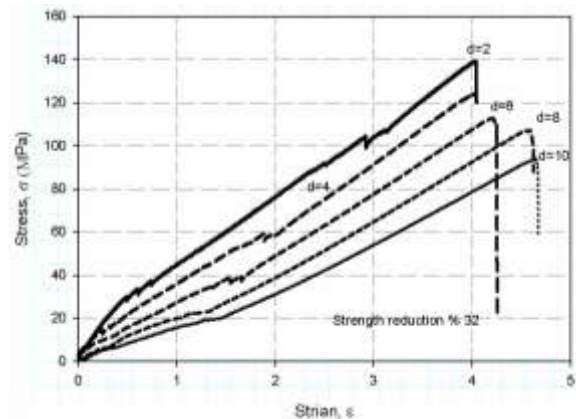


**Fig. 24 Stress strain diagram for [0, 90]<sub>2s</sub> size effect specimen**

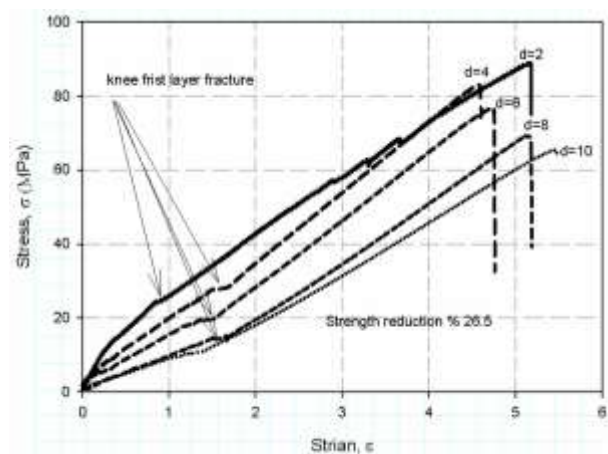


**Fig. 25 Stress strain diagram for [0/45/90]<sub>2s</sub> size effect specimen**

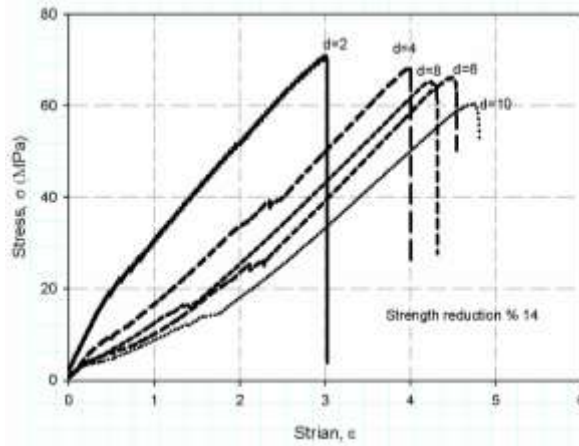


Fig. 26 Stress strain diagram for  $[0/45/90/-45]_s$  size effect specimen

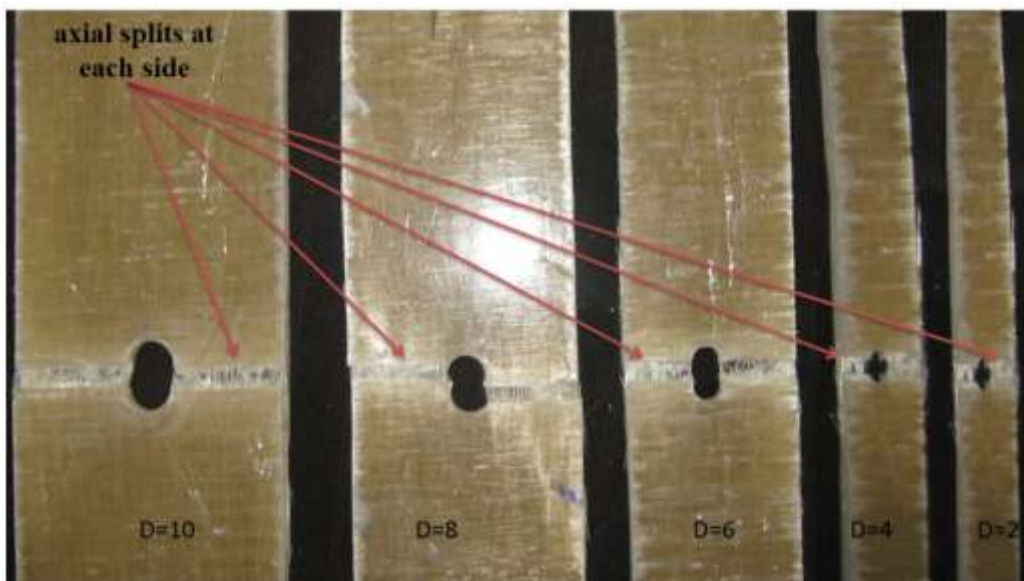


Fig. 27 Post failure image of  $[0/90]_{2s}$

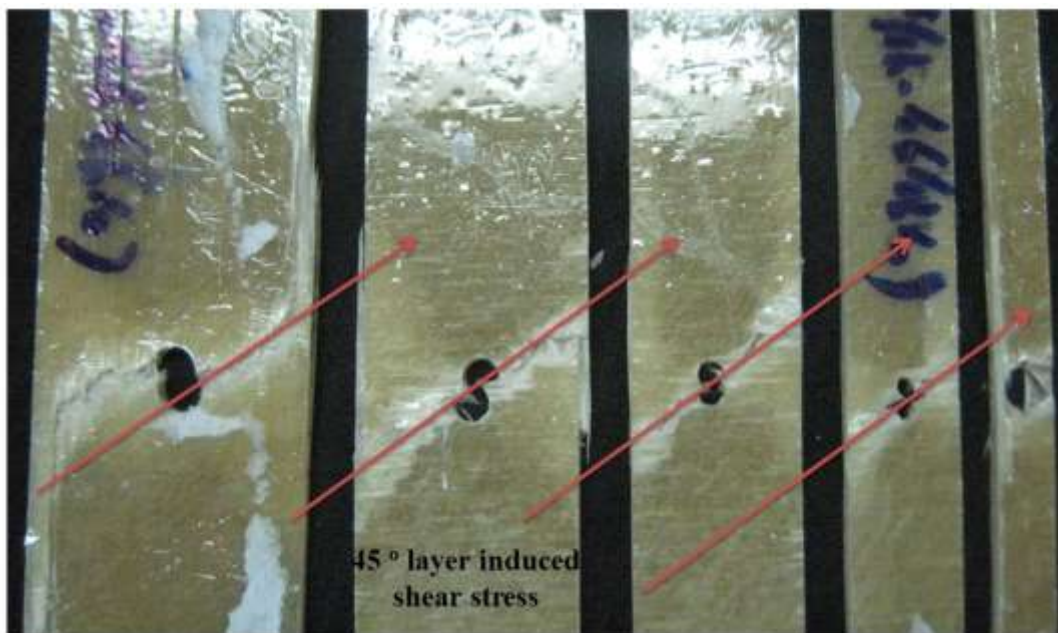


Fig. 28 Post failure image of  $[0/45/90]_{2s}$



Fig. 29 Post failure image of [0, 45, 90, -45]<sub>s</sub>



Fig. 30 through thickness delamination

### Conclusion

The fracture properties of glass fiber composites laminates are measured and following conclusion are summarized:

- Compact tension test specimen is simple and give acceptable results for fiber tension fracture toughness  $G_{Ic}$  of laminates of stacking sequence [0/90]<sub>2s</sub>, as 51.915 kJ/m<sup>2</sup> which agreement with the allowable value in text book. However Center cracked plate specimen is suitable for measuring fracture toughness for Quasi-isotropic laminates [0/45/90]<sub>2s</sub> and [0/45/90/-45]<sub>s</sub> have a value of 32.98 and 31.5 KJ/m<sup>2</sup> respectively.
- A strength reduction of 32 % is observed with increasing the hole diameter from 2 mm to 10 mm, while this percentage was decreasing by inserting an angle ply as 26 % for [0/45/90]<sub>2s</sub> and 14 % for [0/45/90/-45]<sub>s</sub>.
- Delaminations are observed with thickness increasing for un-notched specimens.
- Fiber orientation affects deeply the laminates carrying capacity.
- Three failure modes are summarized for glass fiber composite laminates, fiber pull out, fiber tension and delamination.
- ±45 in plane shear test give acceptable results for shear modulus while underestimates the shear strength value by about 50% when compared with the value measured with the lamination theories.

### References

1. P.P. Camanho, P. Maimi and C.G. Davila, Prediction of size effects in notched laminates using continuum damage mechanics. *Compos. Sci. Technol.*,2007; 67: 2715-2717.
2. J. Lee and C. Soutis, A study on the compressive strength of thick carbon fibre/epoxy laminates. *Composites Science & Technology*, 2007; 67(10): 2015-2026.
3. C. Soutis, "A fiber microbuckling model for predicting the notched compressive strength of composite sandwich panels". *Mechanics of Composite Materials*,2007; 43(1): 51-58.
4. J. Planas, G. V. Guinea, M. Elices, Generalized size effect equation for Quasi-brittle materials, *Fatigue and Fracture of Engineering Materials and Structures*,1997; 20 (5): 671-687.
5. Hassan, Mohammed K., et al. "Prediction of nominal strength of composite structure open hole specimen through cohesive laws." *International Journal of Mechanical & Mechatronics Engineering*. 2012;12 :1-9.
6. Mohammed, Y., Mohamed K. Hassan, and A. M. Hashem. Analytical model to predict multiaxial laminate fracture toughness from 0° ply fracture toughness. *Polymer Engineering & Science*. 2013
7. Pinho, S.T., Robinson, P. and Iannucci, L., Fracture toughness of the tensile and compressive fiber failure modes in laminated composites, *Composites Science and Technology*, 2006; 66:2069-2079.

8. M. V. Donadon, B. G. Falzon, L. Lannucci and J. M. Hodgkinson, Measurement of fiber fracture toughness using an alternative specimen geometry, 16<sup>th</sup> international conference on composite materials, Kyoto, Japan 2007.
9. D. R. Leach, J. C. Seferis, Intrinsic characterization of continuous fiber reinforced thermoplastic composites—1: Toughness characterization of carbon fiber/ polyether ether ketone (CF/PEEK) laminates, *Pure and Applied Chemistry*. 1991; 63 (11):1609–1625.
10. C. Soutis, N. A. Fleck, P. A. Smith, Failure prediction technique for compression loaded carbon fiber-epoxy laminate with an open hole, *Journal of Composite Materials*, 1991; 25:1476–1498.
11. C. Soutis, P. T. Curtis, N. A. Fleck, Compressive failure of notched carbon fibre composites, *Proceedings of the Royal Society London A*. 1993; 241–256.
12. C. Soutis, P. T. Curtis, A method for predicting the fracture toughness of CFRP laminates failing by fiber microbuckling, *Composites Part A* 31. 2000;733–740.
13. Camanho, P. P., and G. Catalanotti. "On the relation between the mode I fracture toughness of a composite laminate and that of a 0° ply: Analytical model and experimental validation." *Engineering Fracture Mechanics* ,2011; 78(13): 2535-2546.
14. Wisnom, M.R., Size effects in the testing of fiber-composite materials. *Compos Sci Technol*. 1999; 59:1937-57.
15. Wisnom, M.R., Khan, B., Hallet, S.R., Size effects in unnotched tensile strength of unidirectional and Quasi-isotropic carbon/epoxy composites. *Composite Structures*.2008; 84:21-28
16. Hitchon, J.W., Phillips, D.C., The effect of specimen size on the strength of cfrp. *Composites*.1978; 9:119-24.
17. Al-Hashem, A., Hasan Tarish, and Gasem Fallatah. "Cavitation erosion behavior of epoxy-, vinyl ester-and phenolic-based fiber glass composites in sea water." *Corrosion*. 2009.
18. Khashaba, U. A. "In-plane shear properties of cross-ply composite laminates with different off-axis angles." *Composite structures*.2004; 65(2): 167-177.
19. Standard test method for tensile properties of polymer matrix composite materials, ASTM D 3039/D 3039M-00. West Conshohocken (PA), USA: American Society for Testing and Materials (ASTM).
20. Jones, R.M., *Mechanics of composite materials*, Taylor&Francis Publication ,1999.
21. Mallick, P.K, *Fiber-reinforced composites*, Marcel Dekker Press, 2nd Edition, 1993.
22. Gibson, Ronald F. *Principles of composite material mechanics*. CRC Press, 2011)
23. Walrath, D. E., and D. F. Adams. "The losipescu shear test as applied to composite materials." *Experimental Mechanics*.1983; 23(1): 105-110.
24. Arcan, M., Z. Hashin, and A. Voloshin. "A method to produce uniform plane-stress states with applications to fiber-reinforced materials." *Experimental mechanics*, 1978; 18(4) :141-146.
25. [ASTM D3518. "Standard Test Method for In-Plane Shear Response of Polymer Matrix Composite Materials by Tensile Test of a±45° Laminate." W. Conshohocken, PA: Am. Soc. Test. Mater., 2001.
26. Standard Method of Test for Plane Strain Fracture Toughness in Metallic Materials, ASTM E399-81, American Society for Testing and Materials, Philadelphia. 1981.
27. C. Soutis, P.T. Curtis and N.A. Fleck, Compressive failure of notched carbon fibre composites. *Proc. R. Soc. London A*, 440 1993: 241-256.
28. Standard, A. S. T. M. "D638M-93, 1993,“." *Standard Test Method for Tensile Properties of Plastics (Metric),” Annual Book of ASTM Standards, Part 8: 59-67.*
29. Davis, Joseph R. *Tensile testing*. ASM International (OH), 2004.
30. T.A.Sebaie, Master thesis,Zagazeg University, Faculty of Engineering, 2006
31. Khashaba, U. A, Tensile and flexural properties of randomly oriented GFRP, *Proc. Of 1<sup>st</sup> Int. Conf. On Mech. Eng. Adv. Tech. For indus. Prod.*, Assiut university, Egypt, 1994; 1(1): 131-143.
32. Jones, Robert M. *Mechanics of composite materials*. Vol. 2. London: Taylor & Francis, 1975.
33. O’higgins, R. M., M. A. McCarthy, and C. T. McCarthy. "Comparison of open hole tension characteristics of high strength glass and carbon fibre-reinforced composite materials." *Composites Science and Technology* ,2008;68(13): 2770-2778.
34. Anderson, Ted L. *Fracture mechanics: fundamentals and applications*. CRC PressI Llc, 2005.